Journal of Cerebral Blood Flow & Metabolism (2012) 32, 1546–1558

www.jcbfm.com

Measurement of 5-HT_{1A} receptor density and *in-vivo* binding parameters of [^{18}F]mefway in the nonhuman primate

Dustin W Wooten[1,2], Ansel T Hillmer[1,2], Jeffrey M Moirano[1,2], Elizabeth O Ahlers[2], Maxim Slesarev[2], Todd E Barnhart[1], Jogeshwar Mukherjee[3], Mary L Schneider[4] and Bradley T Christian[1,2,5]

[1]*Department of Medical Physics, University of Wisconsin-Madison, Madison, Wisconsin, USA;* [2]*Waisman Laboratory for Brain Imaging and Behavior, University of Wisconsin-Madison, Madison, Wisconsin, USA;* [3]*Department of Radiological Sciences, University of California-Irvine, Irvine, California, USA;* [4]*Department of Kinesiology, University of Wisconsin-Madison, Madison, Wisconsin, USA;* [5]*Department of Psychiatry, University of Wisconsin-Madison, Madison, Wisconsin, USA*

The goal of this work was to characterize the *in-vivo* behavior of [^{18}F]mefway as a suitable positron emission tomography (PET) radiotracer for the assay of 5-hydroxytryptamine$_{1A}$ (5-HT_{1A}) receptor density (B_{max}). Six rhesus monkeys were studied using a multiple-injection (M-I) protocol consisting of three sequential bolus injections of [^{18}F]mefway. Injection times and amounts of unlabeled mefway were optimized for the precise measurement of B_{max} and specific binding parameters k_{off} and k_{on} for estimation of apparent K_D. The PET time series were acquired for 180 minutes with arterial sampling performed throughout. Compartmental analysis using the arterial input function was performed to obtain estimates for K_1, k_2, k_{off}, B_{max}, and K_{Dapp} in the cerebral cortex and raphe nuclei (RN) using a model that accounted for nontracer doses of mefway. Averaged over subjects, highest binding was seen in the mesial temporal and dorsal anterior cingulate cortices with B_{max} values of 42 ± 8 and 36 ± 8 pmol/mL, respectively, and lower values in the superior temporal cortex, RN, and parietal cortex of 24 ± 4, 19 ± 4, and 13 ± 2 pmol/mL, respectively. The K_{Dapp} of mefway for the 5-HT_{1A} receptor sites was 4.3 ± 1.3 nmol/L. In conclusion, these results show that M-I [^{18}F]mefway PET experiments can be used for the *in-vivo* measurement of 5-HT_{1A} receptor density.
Journal of Cerebral Blood Flow & Metabolism (2012) **32,** 1546–1558; doi:10.1038/jcbfm.2012.43; published online 4 April 2012

Keywords: 5-HT_{1A}; B_{max}; K_D; [^{18}F]mefway; multiple-injection PET

Introduction

The serotonin 5-hydroxytryptamine$_{1A}$ (5-HT_{1A}) receptor subtype is known to be a critical regulator of the 5-HT system and is believed to have a pivotal role in the pathophysiology of many neuropsychiatric illnesses. 5-hydroxytryptamine$_{1A}$ receptors are expressed both postsynaptically, throughout the forebrain (neocortex and hippocampus), and as a major somatodendritic autoreceptor in the 5-HT neurons of the raphe nuclei (RN). Alterations in the density of 5-HT_{1A} receptors have been implicated in a wide range of neuropsychiatric diseases, based on postmortem histology and animal models. During neurodevelopment, prenatal alcohol exposure has been shown to alter 5-HT_{1A} receptor expression (Druse *et al*, 1991). Positron emission tomography (PET) imaging with 5-HT_{1A}-specific radioligands has a role for providing *in-vivo* assay of receptor density (B_{max}).

The 5-HT_{1A}-specific antagonists currently being used for PET investigation of the 5-HT_{1A} system include [^{11}C]WAY-100635 (Pike *et al*, 1996), [^{18}F]MPPF (Le Bars *et al*, 1998), [^{18}F]FCWAY (Carson *et al*, 2000), and [^{18}F]mefway (Saigal *et al*, 2006), all of which are structurally related to WAY-100635. *In-vitro* measurements of B_{max} have been reported with [^{11}C]WAY-100635 and validated by comparison with its tritiated form (Hall *et al*, 1997), finding high

Correspondence: DW Wooten, Department of Medical Physics, University of Wisconsin-Madison, 1111 Highland Avenue, Madison, WI 53705, USA.
E-mail: dwooten@wisc.edu
This work was supported by NIH grants AA017706, MH086014, AG030524, AA12277, T32CA009206. Additional support was provided by NIH grants S10RR015801, P30HD003352, and S10RR023033.
Received 25 August 2011; revised 11 January 2012; accepted 1 March 2012; published online 4 April 2012

levels of 5-HT_{1A} receptor expression throughout the frontal, temporal, parietal, and cingulate cortices with the highest receptor density in the hippocampus (including regions CA1, subiculum, and uncus). *In-vivo* measurements of 5-HT_{1A} B_{max} in humans have been measured using [18F]MPPF, finding similar rank order in 5-HT_{1A} receptor expression across brain regions as *in-vitro* studies (Costes *et al*, 2002). The *in-vivo* PET assay of B_{max} in humans involves increased experimental complexity compared with typical 'tracer' PET studies, requiring multiple injections of nontracer doses of ligand.

The multiple-injection (M-I) PET technique involves performing serial injections with varying levels of unlabeled ligand, with the intent of occupying a significant fraction of the receptors (Delforge *et al*, 1990). This strategy permits the estimation of B_{max}, separated from the ligand receptor-specific binding parameters (k_{on} and k_{off}). The M-I method provides a measure of receptor density that is independent of the characteristics of the radioligand, unlike the 'binding potential' metric obtained with tracer-only PET studies, which represent a composite function of B_{max} and ligand-receptor affinity (Innis *et al*, 2007). The M-I methods have also been used for the measurement of B_{max} in the peripheral benzodiazepine (Delforge *et al*, 1996), β-adrenergic (Muzic *et al*, 2000; Salinas *et al*, 2007), dopamine transporter (Morris *et al*, 1996; Poyot *et al*, 2001), dopamine D2 (Delforge *et al*, 1999; Christian *et al*, 2004; Mauger *et al*, 2005; Vandehey *et al*, 2010), and nicotinic acetylcholine (Gallezot *et al*, 2008) receptor systems.

The goal of this work was two-fold: (1) to characterize the *in-vivo* kinetic behavior of [18F]mefway and (2) to show its utility for *in-vivo* measurement of 5-HT_{1A} B_{max} using the M-I approach. *In-vitro* and *in-vivo* validation studies with [18F]mefway have shown its high selectivity for 5-HT_{1A} receptors (Saigal *et al*, 2006) and favorable imaging characteristics (Wooten *et al*, 2011a). A more complete characterization of [18F]mefway, measuring radioligand delivery and clearance (K_1 and k_2) and the binding and dissociation rate constants (k_{on} and k_{off}), will provide the necessary information for future experimental design in gauging the detection sensitivity of [18F]mefway to subtle alterations in the 5-HT_{1A} system by disease or mechanistic perturbations in animals and humans. The rhesus monkey serves as a powerful model for studying 5-HT related function, due to its similarities with humans in neurochemical development, anatomy, receptor pharmacology, genetic polymorphisms, neurobehavior, and social structure. In this work, we report the *in-vivo* K_D (K_{Dapp}) of [18F]mefway and 5-HT_{1A} B_{max} in the rhesus monkey. An M-I protocol was used with injections of varying cold masses to decouple the kinetic parameters necessary for estimation of K_{Dapp} and 5-HT_{1A} B_{max}.

Materials and methods

Chemical Synthesis

The synthesis of [18F]mefway (N-{2-[4-(2-methoxyphenyl)-piperazinyl]ethyl}-N-(2-pyridyl)-N-(4-trans-[18F]-fluoromethylcyclohexane)carboxamide) was performed according to previously reported methods (Saigal *et al*, 2006). The average specific activity at the time of first injection of the PET scan was 77 GBq/μmol. The unlabeled mefway used for the M-I studies was purchased from a commercial vendor (Huayi Isotopes, Toronto, ON, Canada) as an 85:15 isomeric mixture of *trans*-mefway to *cis*-mefway. The injected mass for the partial saturation administrations (injection #2) was calculated based on the fractional mass of the *trans*-mefway and the pharmacological effects of the *cis*-mefway component were assumed to be negligible based on our previously reported findings (Wooten *et al*, 2011b).

Design of the Multiple-Injection Experiments

The M-I experiments were designed to optimize the precision of the parameter estimates of B_{max} and the ligand-specific binding parameters (k_{on} and k_{off}). A requirement was placed on the experimental design to limit the first injection to tracer-only doses of [18F]mefway and a duration of 90 minutes before the subsequent injection. This design permits the comparison of [18F]mefway BP_{ND} with other subjects using single-injection protocols acquired at our center. Experimental designs were investigated for 2- and 3-injection studies to select the amount of unlabeled mefway and the injection time for each administration. The experimental design was selected using the D-optimal criterion, which minimizes the correlation between the kinetic parameters (described in Salinas *et al*, 2007). The inverse determinant of the reduced Hessian ($\det(H_R)^{-1}$) is proportional to the volume of the indifference region for the parameter estimates. In minimizing this region, the parameter precision is increased. Only k_{on}, k_{off}, and B_{max} were considered for the optimization. The experimental designs were simulated using the COMKAT software (Muzic and Cornelius, 2001) based on previously measured arterial input functions (Wooten *et al*, 2011*a*) and a range of B_{max} (40 to 100 pmol/mL), k_{off} (0.01 to 0.1 per minute), and k_{on} (0.004 to 0.04 per minute) values estimated from our previous studies and the literature values with comparable ligands (Gunn *et al*, 1998; Hall *et al*, 1997). As a validation of the selected experimental designs, simulated noise was added to each data point of the simulated regions of interest (ROIs) similar to a reported method (Logan *et al*, 2001) using the equation:

$$C_R^* = C_{R(fit)} + \left(G_{(0,1)}c_1\sqrt{C_{R(fit)}} + G_{(0,1)}c_2\right) \quad (1)$$

where C_R^* is the noise-added time-activity curves (TACs) in the different brain regions, $C_{R(fit)}$ is the noise-free TACs, $G_{(0,1)}$ is the noise addition that was a pseudorandom number from a normal distribution with a mean of zero and a standard deviation of 1, and the constants c_1(1.5 to 2.5) and c_2(0 to 60) represent scaling factors to approximate noise found in the original TACs (using 50 realizations).

Parameter estimates were performed on these simulated TACs to examine the parameter identifiability. The optimization was repeated after the first several experiments to incorporate the newly measured parameters in the design of the later experiments.

Positron Emission Tomography Scans

The M-I PET experiments were conducted on a total of six *Macaca mulatta* (rhesus) subjects (2 male and 4 female; 8.2 ± 1.6 kg; 13.0 ± 3.9 years). The subjects were anesthetized for the scans using ketamine (10 mg/kg intramuscularly) and maintained under anesthesia using 0.75% to 2% isoflurane during the course of the experiment. Atropine sulfate (0.27 mg) was administered to reduce secretions. Body temperature, heart rate, breathing rate, and oxygen saturation (SpO_2) levels were monitored and recorded. Catheters were placed in the saphenous vein for administration of ligand and the femoral artery for arterial sampling. Subjects were housed at The Harlow Primate Laboratory at the University of Wisconsin in Madison, which is governed by and strictly adheres to stringent federal statutes and regulations regarding the care and ethical use of laboratory animals. The NIH and USDA oversee the policies and statutes governing the care and ethical use of these subjects. All experimental procedures were approved by the University of Wisconsin Institutional Animal Care and Use Committee.

The PET scans were acquired using a Concorde microPET P4 scanner (Tai *et al*, 2001), which has a detection sensitivity of $\sim 1.2\%$ and in-plane resolution of 2.8 mm as measured using the reconstruction methods for this protocol. Subjects were placed in the prone position in a custom-built stereotaxic headholder. Before injection, a 518-second transmission scan was performed using a ^{57}Co point source. The collection of 3 hours of emission data was initiated with the first bolus injection of [18F]mefway. On the completion of the scan, the subjects were removed from the scanner and returned to their cage when swallowing reflexes were restored and monitored continuously until fully alert.

Measurement of the Arterial Input Function

Arterial samples were collected to provide an input function for kinetic modeling of [18F]mefway. Arterial samples were collected in volumes of 0.5 mL every 10 to 15 seconds for 2 minutes immediately after each injection to every 10 to 20 minutes toward the end of each injection segment. The 0.5-mL whole blood samples were mixed with 50 μL heparinized saline and assayed for radioactivity with a well counter that was cross-calibrated with the PET scanner. The hematocrit was measured to correct for the volume of the heparinized saline present in the extracted plasma. The whole blood samples were then centrifuged for 5 minutes to allow the extraction of 250 μL of plasma, which was added to 50 μL of sodium bicarbonate and assayed for radioactivity. The parent compound was removed from the plasma using two liquid-liquid ethyl acetate extractions as previously reported (Wooten *et al*, 2011*a*).

As implemented, the M-I model requires the [18F]mefway arterial time course to be separated and uniquely defined for each of the three injections. This requires the mathematical removal of radioactivity of the first injection from the second and third injections (and the second injection from the third injection). The first injection was parameterized by fitting the data from 5 to 90 minutes after injection to a biexponential function and extrapolating the curve to the end of the study (3 hours) for subtraction from the subsequent injections. The same method was used to parameterize the second injection, which was then subtracted from the third injection. The individual time courses of [18F]mefway were then decay corrected and divided by the specific activity (at the time of each injection) to yield units of molar concentration (pmol/mL) of mefway that are unaffected by radioactive decay.

Data Analysis

Image Reconstruction: The dynamic list mode emission data were binned into 2 minute sinograms and reconstructed with a filtered back projection algorithm using a 0.5 per cm ramp filter with corrections applied for attenuation, scatter, and scanner normalization. The final matrix size was $128 \times 128 \times 63$, with voxel dimensions of $1.90 \times 1.90 \times 1.21\,mm^3$.

Regions of Interest Selection: Regions of interest were selected from the PET images in cortical areas with uniform 5-HT_{1A} binding. Multiple circular ROIs were placed within the regions of the mesial temporal cortex (MTC) ($0.28\,cm^3$), superior temporal cortex (sTC) ($0.91\,cm^3$), parietal cortex (PC) ($0.91\,cm^3$), dorsal anterior cingulate cortex (dACC) ($0.73\,cm^3$), and the cerebellum (CB) ($0.92\,cm^3$) to extract TACs. The ROIs were also applied to the subcortical region of the RN ($0.08\,cm^3$), guided by the focal uptake of [18F]mefway binding. A denoising algorithm was applied to the dynamic PET images before the extraction of the TACs (Christian *et al*, 2010). The ROIs for these regions are shown in Figure 1.

Parameter Estimation: The *in-vivo* kinetic behavior of [18F]mefway was analyzed using a two-compartment model, as shown in Figure 2, to account for ligand in the free (F) (pmol/mL), including unbound and nondisplaceably bound, and specifically bound (B) (pmol/mL) states. C_{pi} represents the molar concentration of mefway in the plasma (pmol/mL) and serves as the input function. For studies with multiple injections, B and F compartments are created for each injection (i) (Delforge *et al*, 1990; Muzic *et al*, 2000; Christian *et al*, 2004; Morris *et al*, 2004), as described by the differential equations:

$$\frac{dF_i}{dt} = K_1 C_{pi} - k_2 F_i + k_{off} B_i - k_{on} F_i \left(B_{max} - \sum_i B_i \right) \quad (2)$$

$$\frac{dB_i}{dt} = k_{on} F_i \left(B_{max} - \sum_i B_i \right) - k_{off} B_i \quad (3)$$

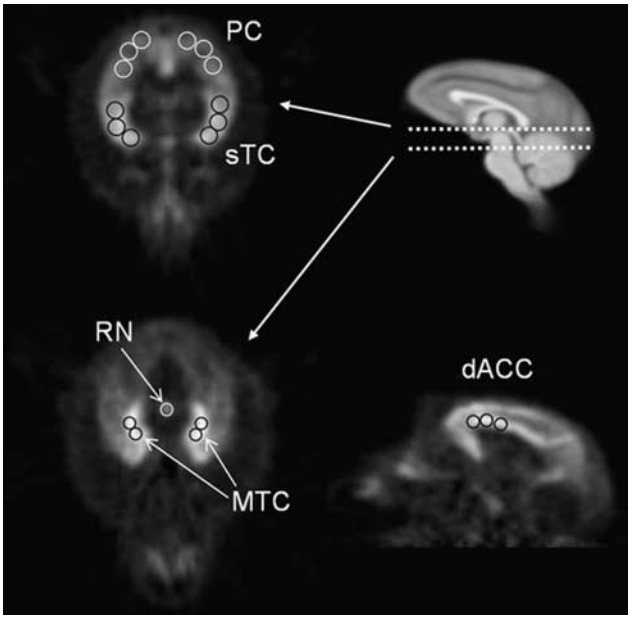

Figure 1 Regions of interest (ROIs) in the areas of the mesial temporal (MTC), dorsal anterior cingulate (dACC), superior temporal (sTC), parietal (PC) cortices, and raphe nuclei (RN) drawn on summed dynamic frames (20 to 90 minutes). The top right sagittal magnetic resonance image illustrates the transaxial planes shown in the two positron emission tomography (PET) images in the left panel and is in the same space as the sagittal PET image (bottom right).

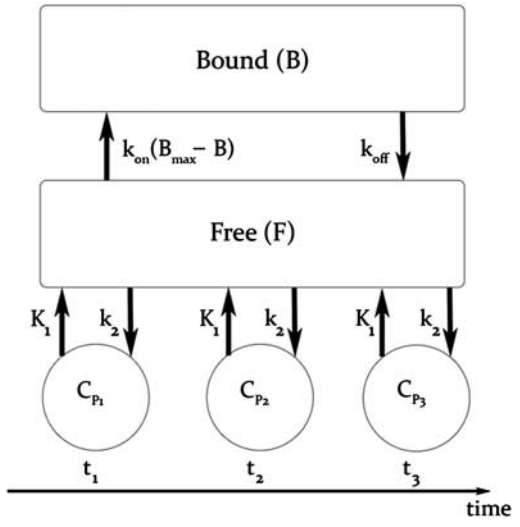

Figure 2 Two-compartment model describing a three-injection protocol. t_{1-3} represent the injection times, C_{P1-3} represent the molar ligand concentration (pmol/mL) in the arterial plasma and bidirectionally exchanged between the free (F) and bound (B) states.

The bidirectional transport of radiotracer across the blood brain barrier, represented by K_1 (mL/min per mL) and k_2 (1/min), dissociation rate constant (k_{off}) (1/min), association rate constant (k_{on}) (1/min), and receptor density (B_{max}) (pmol/mL) are common between each of the injections. The modeled PET signal is obtained by converting the absolute molar concentrations (F_i and B_i) into Bq/cm^3 by multiplication with the time decaying specific activities ($sa_i(t)$) of each injection. The data are then normalized by the frame duration and can be expressed by the following model:

$$C_{PET}(t) = \frac{1}{t_j - t_{j-1}} \times \int_{t_{j-1}}^{t_j} \left\{ \sum_i sa_i(t)(1 - f_V)(F_i(t) + B_i(t)) + f_V A_i \right\} dt \quad (4)$$

The fractional blood volume (f_V) accounts for the vascular component of radioactivity measured in the decaying whole blood (A_i) and was fixed to a value of 0.04 for all brain regions. Thus, the model sums the radioactivity concentration for each injection (i) to obtain the PET signal, C_{PET}, which is not corrected for radioactive decay to be consistent with the acquired PET data.

The parameter estimation for each subject was performed using COMKAT (Muzic and Cornelius, 2001). The following assumptions were implemented to permit the simultaneous estimation of all the regional parameters for [18F]mefway throughout the brain:

(1) Nondisplaceable distribution volume, $V_{ND} = K_1/k_2$, is uniform across all ROIs, whereas K_1 can vary between ROIs to account for regional differences in blood flow.
(2) The specific binding association and dissociation rate constants, k_{on} and k_{off}, are uniform across all ROIs, whereas B_{max} can vary between ROIs.
(3) The blood flow within each ROI does not change throughout the course of the experiment, so the radiotracer influx and efflux constants, K_1 and k_2, are time invariant.

With these assumptions, estimates of k_{on}, k_{off}, and V_{ND} were made uniform for all ROIs and estimates of K_1 and B_{max} were unique for each ROI. For the CB, the compartment for specific binding (B) was not included and only K_1 was uniquely measured for this region. Thus for each subject, a total of 14 parameters were simultaneously estimated from the time series data of 6 brain regions (MTC, sTC, PC, dACC, RN, and CB). The apparent equilibrium dissociation constant, K_{Dapp}, was calculated as: $K_{Dapp} = k_{off}/k_{on}$. The parameter estimates were obtained by minimizing the least squares objective function (o) between $C_{PET}(t)$ and the corresponding ROI measurement (r) for each time frame (j) of the PET scan scaled by a weighting factor (w). Uniform weighting was selected for these data as it has been shown to minimize bias for parameter estimates in PET compartment analysis (Muzic and Christian, 2006). The objective function is described as:

$$o = \sum_{r=1}^{R} \sum_{j=1}^{J} w_{r,j} \left(PET_{r,j} - C_{PETr,j} \right)^2 \quad (5)$$

with six ROIs ($R = 6$) and 180 minutes of PET data in 2 minutes time frames ($J = 90$).

Estimation of uncertainties in the parameter estimates were performed similarly to a method used by Salinas *et al* (2007) and Vandehey *et al* (2010). The parameter estimates obtained from the PET data were used to generate

a noise-free simulated data set for each subject. Noise was then added to the simulated data using the noise model described in equation (1), with 50 noise trials for each subject. Parameter estimates were then obtained for each trial and the standard deviation of each parameter was calculated from the population obtained from the 50 noise trials. The coefficient of variation (cov = s.d./mean × 100%) was then measured for each parameter and mean coefficients of variation were reported for each parameter as the average cov over the six subjects.

For comparison with the B_{max} estimates, measurements were also made for nondisplaceable binding potential, BP_{ND} (Innis *et al*, 2007), using the data from 0 to 90 minutes, consisting of only the high specific activity first injection. BP_{ND} was estimated using the CB as a reference region with the Logan distribution volume ratio (DVR) method and calculated as $BP_{ND} = DVR - 1$ (Logan *et al*, 1996), using a period of linearization of $t^* =$ 40 minutes and a k_2 value obtained from the compartmental modeling.

Results

Optimization of Multiple-Injection Protocol

The optimization of the M-I protocol focused on selecting the unlabeled dose of mefway for the second and third injections and the timing of the third injection. It was found that identifiability of B_{max}, k_{on}, and k_{off} was most sensitive to the mefway dose for the second injection and much less sensitive to the timing and dose of the third injection (see Discussion and Figure 3). Figure 3 illustrates the dependence of the $\det(H_R)^{-1}$ on the mefway dose for the second injection, suggesting the optimal dose is ~100 to 200 nmol. Also shown is the B_{max} correlation with k_{on} and k_{off}, showing that the high correlation is reduced at an optimal range of unlabeled mass doses for the second injection. The sensitivity curves in the region of the MTC for B_{max}, k_{on}, and k_{off} (shown in Figure 3) illustrate the decoupling of the parameters over the duration of the experiment.

The experimental protocols for subjects M1 to M6 are shown in Table 1. It should be noted that the initial optimizations were based on a K_{Dapp} that was ~70% lower than the newly measured values. Analysis from the first subject showed that optimal parameter estimation needed only a high mass dose in injection 2 and low mass in injection 3, which was then implemented in the following studies. As the experiments progressed, the most recent parameter estimates were incorporated into the optimization and resulted in increasing the mefway mass for the second injection.

Measurement of k_{on}, k_{off}, and B_{max}

The parameter estimates for all of the subjects are given in Table 2, including a single estimate for k_{on}, k_{off}, and V_{ND} across all regions and individual ROI estimates for K_1 and B_{max} in the MTC, sTC, PC, dACC, and RN. For these regions, the highest 5-HT_{1A} receptor density was found in the MTC and dACC, with intermediate levels in the sTC and RN, and lower receptor expression in the PC. The average (over brain regions) cov in B_{max} was 17.9% across the six subjects. Of the estimated parameters, k_{on}

Table 1 Injection parameters for multiple-injection (M-I) experiments

Injection#	*Parameter*	*Subject*					
		M1	*M2*	*M3*	*M4*	*M5*	*M6*
1	Time (minutes)	0	0	0	0	0	0
	Activity (MBq)	58.1	66.2	63.3	61.8	64.8	57.7
	Mass (nmol)	2.4	0.5	0.8	0.8	1.2	0.6
2	Time (minutes)	91	90	90	90	91	90
	Activity (MBq)	60.3	61.0	57.4	60.0	51.4	58.8
	Mass (nmol)	19.2	30.6	175.5	164.1	141.1	134.6
3	Time (minutes)	150	120	130	130	131	130
	Activity (MBq)	46.3	65.9	61.0	55.1	59.6	58.1
	Mass (nmol)	113.6	1.1	1.7	1.5	2.4	1.4

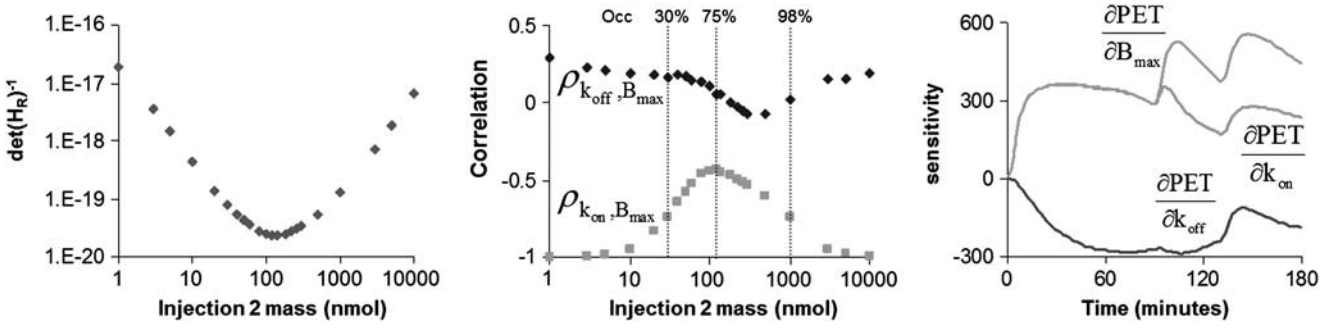

Figure 3 Experimental design—effects of mass in the second injection. (Left) D-optimal inverse determinant of the reduced Hessian ($\det(HR)^{-1}$) criterion as a function of injected mass. (Middle) Correlation between B_{max} with k_{on} and k_{off} as a function of injected mass. (Right) Sensitivity curves for k_{on}, k_{off}, and B_{max} in the mesial temporal cortex (MTC) in which the second injection consists of unlabeled mefway mass that occupies ~75% of the available receptors. PET, positron emission tomography.

Table 2 Parameter measurements across regions

Region	*Parameter*	*Units*	*M1*	*M2*	*M3*	*M4*	*M5*	*M6*	*Mean*	*s.d.*
All ROIs excluding CB	k_{on}	1/min	0.0082	0.0066	0.0057	0.0079	0.0076	0.0059	0.0070	0.0010
	k_{off}	1/min	0.024	0.028	0.029	0.024	0.028	0.039	0.029	0.005
	K_D	pmol/mL	3.0	4.2	5.1	3.1	3.6	6.6	4.3	1.3
All ROIs	V_{ND}	unitless	3.7	3.3	3.5	2.4	2.2	2.2	2.9	0.6
CB	K_1	mL/mL per minute	0.62	0.36	0.68	0.28	0.80	0.29	0.50	0.20
MTC	K_1	mL/mL per minute	0.70	0.59	0.83	0.50	0.46	0.55	0.60	0.13
	B_{max}	pmol/mL	42.3	29.3	54.8	36.6	38.0	47.8	41.5	8.2
sTC	K_1	mL/mL per minute	1.01	0.67	0.95	0.51	0.51	0.48	0.69	0.22
	B_{max}	pmol/mL	21.6	21.0	29.8	21.3	20.2	28.1	23.7	3.8
PC	K_1	mL/mL per minute	1.03	0.65	0.69	0.40	0.47	0.35	0.60	0.23
	B_{max}	pmol/mL	14.2	11.2	13.3	11.7	10.9	15.5	12.8	1.7
dACC	K_1	mL/mL per minute	1.16	0.68	1.01	0.48	0.50	0.42	0.71	0.28
	B_{max}	pmol/mL	33.8	30.4	50.1	30.1	28.6	43.9	36.1	8.0
RN	K_1	mL/mL per minute	1.00	0.80	1.05	0.51	0.48	0.63	0.74	0.22
	B_{max}	pmol/mL	18.8	17.6	18.2	14.8	19.0	26.6	19.2	3.6

MTC, mesial temporal cortex; sTC, superior temporal cortex; PC, parietal cortex; dACC, dorsal anterior cingulate cortex; CB, cerebellum; RN, raphe nucleus; ROI, region of interest.
The coefficients of variation (*cov* = *s.d./mean* × *100*) for each estimated parameter found using Monte Carlo methods, resulted in uncertainties of: k_{on} (4%), k_{off} (4%), K_D (6%), V_{ND} (2%), K_1 in the CB (4%), MTC (4%), sTC (4%), PC (5%), dACC (4%), RN (4%), B_{max} in the MTC (3%), sTC (4%), PC (4%), dACC (3%), and RN (4%).

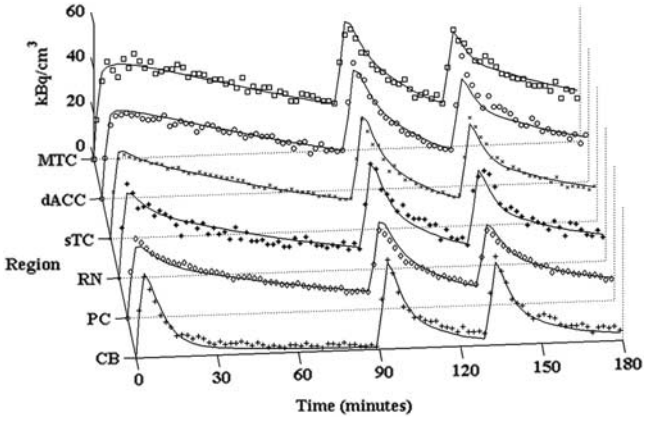

Figure 4 Measured time-activity curves (not corrected for decay) and model predictions (solid line) for subject M4 in the regions of the MTC (□), dACC (○), sTC (×), RN (*), PC (◇), and CB(+). MTC, mesial temporal cortex; sTC, superior temporal cortex; PC, parietal cortex; dACC, dorsal anterior cingulate cortex; CB, cerebellum; RN, raphe nucleus.

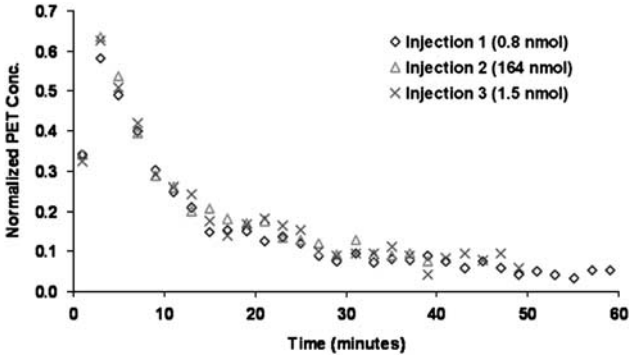

Figure 5 Cerebellum time-activity curves (not corrected for decay) for three injections in subject M4 (Bq/mL/i.d. × 1,000). The data for injection 2 and injection 3 were corrected for residual activity present from the previous injection(s) by subtracting the extrapolated activity using a biexponential function. PET, positron emission tomography.

displayed the lowest variability across this group of subjects, with a *cov* of 14%. There was slightly higher variability in k_{off} (*cov* = 17%), which resulted in a *cov* = 29% in K_{Dapp} due to the propagation of errors. The average K_{Dapp} of [18F]mefway for the 5-HT_{1A} receptor site was 4.3 ± 1.3 pmol/mL.

Figure 4 displays the PET measured time courses and the model output for the regions of the MTC, dACC, sTC, RN, PC, and CB in one subject. The CB is also shown separately in Figure 5 to illustrate the absence of measurable 5-HT_{1A} binding in this region, with each of the three injections superimposed over a single time course after correction for residual activity from previous injection(s).

Discussion

In our previous work, we reported a direct comparison of the *in-vivo* behavior of [18F]mefway with two other 5-HT_{1A} receptor antagonists, [11C]WAY-100635 and [18F]MPPF, under single-bolus injection conditions (Wooten *et al*, 2011*a*), thus these experiments were not designed for the direct measurement of K_D. In the work presented herein, a K_{Dapp} of 4.3 ± 1.3 nmol/L was measured when averaged over the six subjects, which is similar to *in-vivo* measures for other related 5-HT_{1A} PET antagonists. Farde and colleagues (1997) performed a PET study of [11C]WAY-100635 in a single cynomolgus monkey using varying mass injections with competing

drug and reported a K_{Dapp} of ~1 to 2 nmol/L (estimated from the figure). A recent study was conducted using [18F]FPWAY in 21 rhesus monkeys and reported apparent K_{Dapp} values ranging from 1 to 4 nmol/L (*cov* ~ 30% using s.e.m.) in rhesus monkeys (Spinelli *et al*, 2010). For [18F]MPPF, M-I studies were performed in humans ($n = 5$) and reported $K_{Dapp} = 2.8$ nmol/L (*cov* ~ 50%) (Costes *et al*, 2002), yielding comparable results with [18F]mefway. This similarity in the 5-HT_{1A} affinity of [18F]MPPF and [18F]mefway is not consistent with our previous results, which suggested that the K_{Dapp} for [18F]mefway is approximately three-fold lower compared with [18F]MPPF based on BP_{ND} comparisons (Wooten *et al*, 2011*a*) and *in-vitro* measures (Khawaja *et al*, 1995; Saigal *et al*, 2006). This discrepancy in magnitude between the compounds may be due to differences in species, nonspecific binding in the brain (f_{ND}), or experimental design. However, the lower K_{Dapp} values reported for [18F]MPPF were accompanied by reduced estimates of B_{max} (discussed below), indicating a degree of compatibility with our results within the context of the ratio of B_{max}/K_{Dapp}.

In-Vivo Measurement of 5-HT_{1A} B_{max}

The highest values of B_{max} were measured in the regions of the MTC and dACC. Due to the limited resolution of PET assay and the lack of accompanying magnetic resonance imaging scans, only large areas with uniform binding of each specific brain region were selected for analysis. *In-vitro* autoradiography measurements in the hippocampus of the cynomolgus monkey reveal a heterogeneous distribution of 5-HT_{1A} receptors across the hippocampal subfields, with highest binding in the area dentata, subiculum, and parasubiculum in the range of 50 to 100 fmol/mg of protein (Köhler *et al*, 1986). In humans, post mortem *in-vitro* studies using [3H]WAY-100635 have shown high levels of receptor density in the hippocampus areas ranging from 31 fmol/mg of wet tissue in the parahippocampus to 113 fmol/mg of wet tissue in the hippocampus CA1 pyramidal layer (Hall *et al*, 1997). A separate study also using [3H]WAY-100635 found 5-HT_{1A} receptor densities of 200 to 300 fmol/mg of wet tissue in the CA1 of the hippocampus (Burnet *et al*, 1997). We measured an average B_{max} value of ~40 pmol/mL in the MTC, which included regions of the hippocampus. These *in-vivo* measurements of B_{max} are significantly lower than those obtained with the *in-vitro* assay. The direct comparison of *in-vitro* and *in-vivo* PET assay is challenging due to high degree of spatial averaging with PET, which will result in an underestimation of B_{max} for structures with cross-sectional areas that are comparable to the scanner resolution (< 2 to 4 mm). An example of this effect is most profound when considering the small focal structure of the RN. Reported *in-vitro* receptor densities in the dorsal raphe in humans range from 50 fmol/mg of wet tissue to 230 fmol/mg of wet tissue (Burnet *et al*, 1997; Hall *et al*, 1997) compared with our measured densities in the raphe of 18.1 ± 4.3 pmol/mL. The *in-vivo* measurements we report are not specific to just the dorsal region of the RN, but selected as the focal region in the superior PET images of the midbrain region. There was no attempt to correct for the resolution related partial volume effects of this region and we acknowledge that the reported B_{max} in the RN is likely underestimates of those that would be obtained with autoradiography. However, we do not believe that this invalidates an intersubject comparison of (*in vivo*) PET measures in the region of the RN, assuming that the partial volume correction is consistent for all subjects. Because this correction accounts not only for regional size of brain structures but also for the spill over (and spill in) of the radioligand signal from surrounding regions, consideration must be given to variations in brain and body size of the subjects being compared. The subjects in this work were all fully grown adults of comparable weight (8.2 ± 1.6 kg) and age (13.0 ± 3.9 years), however, partial volume correction may be needed in experimental designs having greater variability in brain size (e.g., comparing early adolescent with adults subjects).

There have been several studies reporting *in-vivo* PET measures of 5-HT_{1A} receptor densities using a variety of equilibrium and M-I techniques with PET radioligands. In a cynomolgus monkey, B_{max} values of ~16 and 5 pmol/mL were found in the neocortex and RN, respectively, using a 2-injection protocol with [11C]WAY-100635 (Farde *et al*, 1997). A more recent study in juvenile rhesus monkeys ($n = 21$) found B_{max} values of 5 to 13 pmol/mL (*cov* ~ 26% using s.e.m.) and 1 to 2 pmol/mL (*cov* ~ 34% using s.e.m.) in the hippocampus and RN, respectively, using a 2-point bolus plus constant infusion equilibrium protocol with [18F]FPWAY (Spinelli *et al*, 2010). Both of these previous studies used scatchard graphical analysis to estimate B_{max}, which has been shown to be a valid technique with PET measurements, although high uncertainty in B_{max} estimation can be seen if there is insufficient receptor occupancy for the partial saturation injection (Holden and Doudet, 2004). This may explain some of the variation between results, with experiments using [18F]FPWAY achieving only 40% occupancy. In humans, M-I PET studies were performed with [18F]MPPF, finding B_{max} values of 2.9 pmol/mL (*cov* ~ 50%) in the hippocampus (Costes *et al*, 2002) using a 2-injection (nonequilibrium) protocol. This is a 10-fold difference in measured B_{max} compared with the values reported herein. This discrepancy in B_{max} may be attributed in part to species differences; however, it may also be the result of methodological differences with the level of receptor saturation achieved for the experiments, which is discussed in the section below.

Considerations in Experimental Design

Careful attention must be given to the experimental design in M-I studies to ensure identifiability of each individual parameter, particularly between k_{on} and B_{max}. Generally, parameter estimation algorithms will yield combinations of B_{max} and k_{on} estimates that accurately model the experimental data, even in the case of a faulty experimental M-I design. In such situations, it is the product, $k_{on} \cdot B_{max}$, that is identified and not the independent measures of either parameter. For this work, the D-optimal criterion (which minimizes the indifference region and increases parameter precision) was used to assess the measured precision of the binding parameters k_{on}, B_{max}, and k_{off} and to determine the required experimental design for identifying each. It should be noted that the 3-injection design implemented in this protocol was not selected based on the criteria of experimental simplicity (i.e., the shortest scan with fewest injections). The requirement was enforced that the first injection of each study consist of high specific activity [18F]mefway and 90 minutes of scanning. It has been shown that for other applications, it is possible to measure B_{max} with a 2-injection protocol with partial saturating doses of the ligand for the first injection (Salinas *et al*, 2007). Such a design foregoes the ability to measure BP_{ND} for comparison with radiotracer-only scans and was therefore not investigated for this work. Figure 3 illustrates the relation between one of the experimental variables (unlabeled mefway mass for the second injection) with the D-optimal metric and the effects on the measured output parameters and sensitivity curves. The correlation of k_{off} with B_{max} ($\rho_{k_{off},B_{max}}$) remains small (<0.3) across all values of injected mass, suggesting their relation is not exclusively dependent on the mefway dose, but improvement in decoupling these parameters could be achieved over a range of competing doses of mefway. The variability of the measure k_{off} across subjects was relatively low, 0.030 ± 0.005 per minute ($cov = 17\%$), which is attributed to its high identifiability for this experimental design. The correlation between k_{on} and B_{max} ($\rho_{k_{on},B_{max}}$) revealed much greater dependence on the amount of competing mefway. As expected from radiotracer studies and illustrated in Figure 3, there is complete correlation between the parameters($\rho_{k_{off},B_{max}} = -1$) in the absence of significant mefway dose. This correlation can be significantly reduced by increasing the competing mefway in the second injection, with a minima in correlation corresponding to receptor occupancy of $\sim 75\%$.

An examination of the sensitivity curves, $\partial \mathrm{PET}(t)/\partial\theta_i$, where θ_i represents an estimated parameter, graphically illustrates the decoupling of the parameters. Figure 3 shows the scaled sensitivity curves for B_{max}, k_{on}, and k_{off}. Complete coupling between k_{on} and B_{max} can be seen in the sensitivity curves before injection 2 where curves overlay. In the case where partial receptor saturation occurs (receptor occupancy $\sim 75\%$), there is a divergence of the sensitivity curves for k_{on} and B_{max}, indicating a reduction in the covariance. The sensitivity curves illustrate that identification of k_{on} and B_{max} comes primarily from injection 2, and additional decoupling of k_{off} from k_{on} and B_{max} comes from the third injection.

Examination of the D-optimal criteria, as seen in Figure 3, shows that the decoupling of k_{on} and B_{max} is increased with increasing mefway mass (up to a limit) with an occupancy range optimal for decoupling being 50% to 96% of the 5-HT_{1A} receptor sites. This finding that higher receptor occupancy is optimal to uncouple k_{on} and B_{max} is comparable to that of a previous 2-injection M-I study using [18F]-(S)-fluorcarazalol for measuring B_{max} of myocardial β-adrenergic receptors, which found receptor occupancies of $\sim 90\%$ were optimal for precise estimation of receptor concentration (Salinas *et al*, 2007). For our implementation with three injections, we found maximum decoupling of k_{on} and B_{max} occurred with a saturating dose of $\sim 75\%$ receptor occupancy, corresponding to a dose, averaged over the six subjects, of ~ 12 nmol/kg. The peak occupancies observed for subjects M1 to M6 were 95, 43, 93, 93, 91, and 73% respectively, from the high dose mefway injections. We compare these occupancies with an M-I study in humans using [18F]MPPF (Costes *et al*, 2002), which administered MPPF doses of ~ 20-fold (estimated) lower than doses used in this work. Based on our simulations with mefway, unlabeled dose at this level would not be adequate to decouple k_{on}, k_{off}, and B_{max}, resulting in instability of the parameter estimates. This large difference in occupancy levels may explain the discrepancies in the 5-HT_{1A} B_{max} estimates between methods.

The peak transient occupancy of the 5-HT_{1A} receptors as a function of mefway dose is shown in Figure 6. This relation is based on the measured *in-vivo* parameters of the six subjects and the error bars represent the standard deviation accounting for the variations in the parameters as well as the differences in [18F]mefway observed in the measured input function. This information can be used as a guide for examining mass effects in radiotracer-only studies. For a [18F]mefway synthesis yielding a specific activity of 111 to 185 GBq/μmol (3,000 to 5,000 mCi/μmol) and a 111-MBq (3 mCi) injection (typical of our tracer-only single-bolus injection studies), the 5-HT_{1A} receptor occupancy will range from 1.0% to 1.6%. Under these conditions, it will be possible to perform two sequential radiotracer studies on different subjects, from the same batch (i.e., synthesis) of [18F]mefway, without exceeding a threshold of 4% to 5% receptor occupancy from unlabeled mefway at 'tracer' levels.

The analysis for the parameter estimations involved several assumptions that require consideration. The blood flow was assumed to be constant over the course of the 3-hour experiment. Potential alterations in blood flow would change the rate of

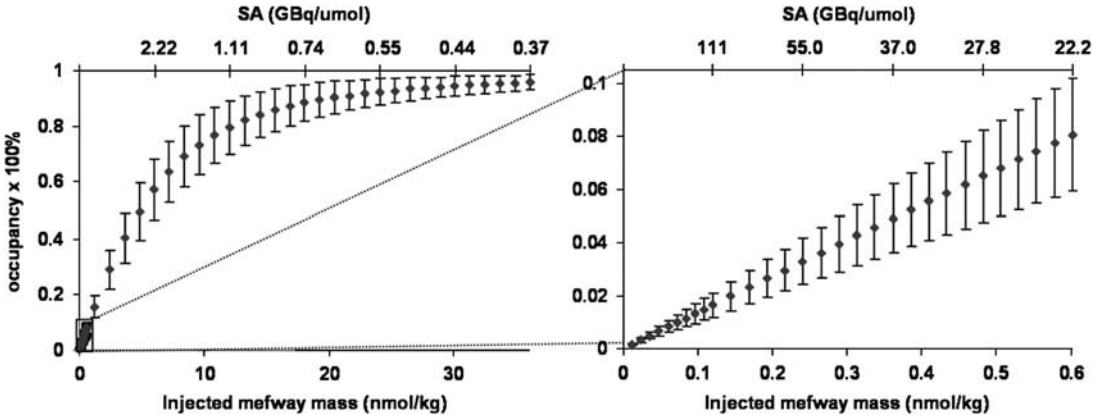

Figure 6 Receptor occupancy as a function of injected mass (nmol/kg) and specific activity when using the average parameter values. The intersubject standard deviation is shown by the error bars, which illustrate the difference seen among subjects due to the individual parameters and subject weights. The bottom axis shows the injected mass in nmol/kg and the top axis shows the specific activity (SA) in GBq/μmol (assuming a 111-MBq (3 mCi) injection typical to our tracer-only single-bolus injection studies). The left image shows the receptor occupancy in the full range from high specific activity to near saturation. The right image shows the receptor occupancy in the mass range of a typical high specific activity injection.

mefway delivery (via K_1) and efflux (via k_2) and bias the measurement of these parameters. The heart rates of the subjects were monitored throughout the studies and showed a gradual decreasing trend during the course of the experiment, with a total decrease of $\sim 20 \pm 5\%$ for the 3-hour scan. There was no observable change in heart rate, SpO_2 levels, or breathing rate when the saturating dose of mefway was delivered. Although this does not discount the possibility of changes to cerebral blood flow, it does alleviate the concern that global changes were induced by the mefway drug. The model included a separate K_1 for each region to account for regional differences in ligand delivery; however, the assumption was made that the nondisplaceable volume of distribution (V_{ND}) remains constant across all examined brain regions. This assumption is consistent with reference region methods of analysis for single injection PET studies. Further, this constraint can accommodate regional perfusion changes, as it has been shown that V_{ND} remains constant under conditions of changing blood flow (Logan *et al*, 1994). The assumption of uniform V_{ND} across regions was examined by fitting each region independently and allowing k_2 to float with the other parameters to determine the effects on the resulting B_{max} and V_{ND} estimates. Minimal change in B_{max} ($\sim 1\%$) and V_{ND} ($\sim 5\%$) was observed in the high density 5-HT_{1A} receptor region of the MTC. However, in the lower density 5-HT_{1A} receptor region of the PC, a negative correlation between V_{ND} and B_{max} was observed leading to an increase of $\sim 19\%$ for B_{max} and a decrease of $\sim 18\%$ for V_{ND} when averaged over all subjects. Thus, any potential bias introduced by the assumption of constant V_{ND} would surface primarily in the low 5-HT_{1A} receptor density regions.

As configured, implementation of the M-I model required separate arterial input functions for each injection, defined in units of molar concentration of mefway (pmol/mL). Separation of the input functions involved extrapolating data from previous injection(s) and subtracting from the subsequent injection(s), with a biexponential function

$$\left(d_1 e^{-\lambda_1 t} + d_2 e^{-\lambda_2 t}\right)$$

used for the extrapolation. This was necessary to account for residual activity from previous injections. At 30 minutes after injection 2, the radioactivity from injection 1 still accounted for $\sim 15\%$ of the total parent radioactivity in the plasma and at 30 minutes after injection 3, injections 1 and 2 accounts for $\sim 27\%$ of the total plasma activity. The fitting of the second injection to a biexponential function was problematic because it consisted of only 40 minutes of arterial sampling time before the administration of the third injection. We initially explored the use of a scaled (by injected activity) version of the first injection for the subsequent injections based on the assumption that each injection would have similar a time course. However, close examination of the input functions revealed the second injection possessed a broader peak (i.e., smaller λ_1), suggesting an alteration in the radiotracer delivery between injections. It is speculated that the addition of pharmacological doses of unlabeled mefway increased the bioavailability of [18F]mefway in the system, possibly by releasing previously bound [18F]mefway from the receptors and by preventing new radiotracer from binding. It was initially assumed that small inaccuracies in the extrapolated function fitted to 40 minutes or less of arterial sampling data, coming from the second injection, would result in large variation in the binding parameter estimates due to the presence of the unlabeled mefway in this injection. To examine the effects of potential inaccuracies in the input function of the second injection, the data were analyzed with two different extrapolation schemes.

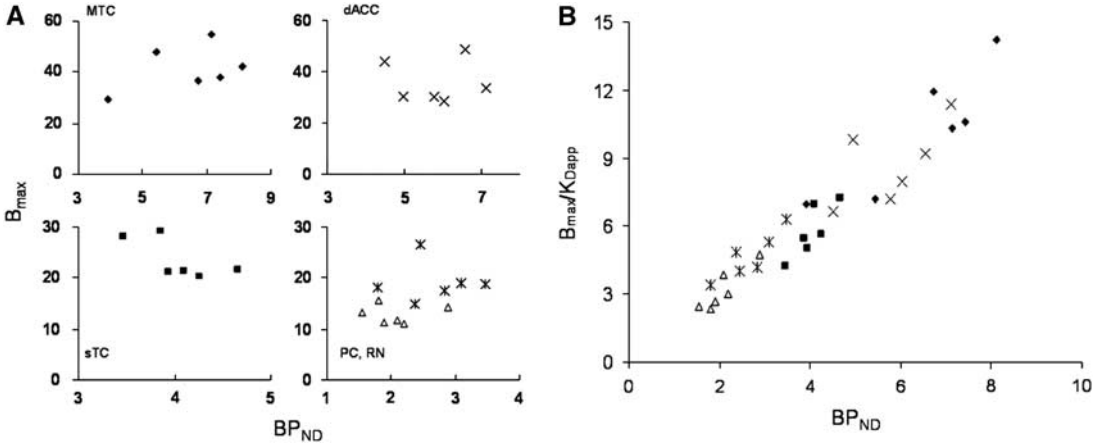

Figure 7 (**A**) Comparison of B_{max} with BP_{ND} in the regions of the MTC (♦), dACC (×), sTC (■), RN (✱), and PC (△). (**B**) Comparison of B_{max}/K_{Dapp} with BP_{ND} for all subjects across brain regions. MTC, mesial temporal cortex; sTC, superior temporal cortex; PC, parietal cortex; dACC, dorsal anterior cingulate cortex; RN, raphe nucleus.

The range of variation was determined from the input function of injection 1, first using the entire 90-minute time course and a second using only the data out to 40 minutes. The percent difference in the biexponential decay parameters (λ_1 and λ_2) was typically $<20\%$ between methods; however, in one study, there was a 44% difference in λ_2 (the slow decay term). This difference was then incorporated into the extrapolated data for the second injection to examine the effects of inaccurate extrapolation on the outcome variables B_{max} and K_{Dapp}. It was found that B_{max} varied by $<1.5\%$ in all areas and K_{Dapp} varied by $<1.3\%$, suggesting that the experimental design is relatively insensitive to the concentration of mefway and its time course once the third injection is administered, as illustrated by the sensitivity curves for B_{max} and k_{on}.

The unlabeled mefway used in these experiments was a commercially purchased reference standard consisting of an isomeric mixture of *cis*- and *trans*-mefway (15:85). We have recently shown that *cis*-[18F]mefway exhibits low, but significant 5-HT_{1A} binding compared with *trans*-[18F]mefway, with a BP_{ND} in the MTC of 0.58 and 7.70 for *cis*- and *trans*-[18F]mefway, respectively (Wooten *et al*, 2011*b*). This profound difference in the binding affinity of isomeric pairs has been reported for other 5-HT_{1A} PET radiotracers (Lang *et al*, 1999; Wilson *et al*, 1999). In this work, the reported injected masses are based only on the measured *trans*-mefway mass and exclude the *cis*-mefway mass fraction. The presence of unlabeled *cis*-mefway in the high dose injections of mefway are assumed to cause negligible effect. It can be approximated, from our previously reported binding potentials for *cis*- and *trans*-[18F]mefway (Wooten *et al*, 2011*b*), that for equal *cis*- *and trans*-concentrations, the *cis*-mefway would represent 7.6% (0.58/7.70) of the bound mefway, which suggests that only $\sim$1% of the receptor sites are occupied by the *cis*-isomer for the mixture used in this work.

BP_{ND} as an Index for B_{max}

The first 90 minutes of each study was used as a baseline to extract BP_{ND} estimates for comparison with direct measurements of B_{max} and K_{Dapp}. The outer cortex in the lobes of the CB was used as the reference region for the BP_{ND} estimation. We have previously reported on the use of the CB as a region with negligible 5-HT_{1A} binding for radiotracer [18F]mefway studies (Wooten *et al*, 2011*a*). The lack of measurable specific binding was confirmed in this study, revealing no measurable displacement of [18F]mefway in the CB as illustrated in Figure 5. Shown in Figure 7A are scatter plots of the measured B_{max} values with the BP_{ND} for the ROI data across subjects. Regression analysis found no significant correlation between B_{max} and BP_{ND} for any of the regions: MTC ($P=0.3$), dACC ($P=0.98$), sTC ($P=0.14$), PC ($P=0.83$), and RN ($P=0.99$). However, significant correlation was found between BP_{ND} and B_{max}/K_D in all regions (MTC ($P=0.014$), sTC ($P=0.017$), PC ($P=0.0065$), and RN ($P=0.023$)) with the exception of the dACC ($P=0.15$). These data are shown in Figure 7B with all of the regions plotted on the same axis (although they were analyzed separately). A similar lack of correlation between the dopamine transporter B_{max} and a composite binding parameter (BP_P) has been reported using [11C]cocaine and serial equilibrium PET studies (Logan *et al*, 1997). The authors attributed the absence of correlation to a lack of robustness in their estimation of B_{max}. A significant positive correlation has been reported between BP_{ND} and B_{max} values as well as BP_{ND} and B_{max}/K_{Dapp} in extrastriatal dopamine D_2 receptors using [11C]FLB457 and a scatchard type multiscan session (Olsson *et al*, 2004). In this particular work, however, a correlation was also observed between B_{max} and K_{Dapp} that may contribute to the correlation observed between B_{max} and BP_{ND}. Additionally, the data were regressed across subjects and across regions whereas our analysis is not

regressed across brain regions. It has been suggested that nonequilibrium experiments, such as M-I designs which decouple B_{max} and k_{on}, may improve the identifiability of B_{max} (Morris *et al*, 1999). For the data reported herein with six subjects, the mean *cov* of B_{max} across the ROIs was 17.9% which was similar to the mean *cov* of the BP_{ND} values of 17.3%, suggesting that the same variability is seen in the binding indices and neither exhibits an advantage in precision of parameter estimation. The data in Figure 7 suggest that BP_{ND} is not a representative proxy of the receptor density (B_{max}) across subjects, but can serve as an index of B_{max}/K_{Dapp}. We neither attempt to generalize this statement for all PET neuroligands and neuroreceptor systems nor attempt to explain this relation of B_{max} and BP_{ND} based on the methodological approaches that were used, as these issues have been discussed in the literature (Morris *et al*, 1999; Olsson *et al*, 2004) and remain largely unresolved.

All *in-vivo* PET methods for B_{max} and K_{Dapp} measurement, equilibrium and nonequilibrium, use assumptions that can potentially bias the outcome measures. In this work, K_{Dapp} was fixed as a constant across all ROIs by estimating only a single k_{on} and k_{off} for each subject. This was performed primarily to reduce the number of estimated parameters and in turn enhance the identifiability of the others. K_{Dapp} is sensitive to several factors that may challenge this assumption, such as endogenous 5-HT competition within the vicinity of the receptors. The effects of competing neurotransmitter on the measured K_{Dapp} are given as $(K_{Dapp})^{est} = (K_{Dapp})^{0}(1 + F_{5HT}/K_{D}^{en})$, where $(K_{Dapp})^{est}$ is the measured K_{Dapp} in the presence of endogenous 5-HT (as measured in these experiments), $(K_{Dapp})^{0}$ is the measured K_{Dapp} in the absence of 5-HT, F_{5HT} is the synaptic concentration of 5-HT, and K_{D}^{en} is the equilibrium dissociation constant of 5-HT (Delforge *et al*, 2001). This relation suggests that 50% occupancy of the receptors by endogenous 5-HT will result in a doubling of $(K_{Dapp})^{est}$ compared with conditions under 5-HT depletion. By imposing a single K_{Dapp} across all brain regions (i.e., ROIs) for each subject, we assume uniform 5-HT occupancy across regions. We also assume no temporal change in endogenous 5-HT due to anesthesia during the course of the experiments. Although no effects on endogenous 5-HT due to ketamine have been measured (Bacopoulos *et al*, 1979), isoflurane has been shown to reduce endogenous 5-HT levels (Tokugawa *et al*, 2007). To minimize potential variations in 5-HT across the cohort, all subjects were anesthetized with the same methodology and consistent timing was used for the injections. The vital signs were examined for evidence of physiological changes. SpO_2 levels remained constant throughout the scanning procedure and were relatively similar between subjects with mean and standard deviation of 98.6 ± 0.6% saturation. Breathing rate was within a range of 10 to 20 breaths/minute, and did not reveal a noticeable trend in variation from beginning to end of the scanning procedure. The average breathing rate among all subjects was 15.1 ± 2.3 breaths/minute.

Further, 5-HT depletion and competition experiments will be required to fully validate the use of a uniform K_{Dapp} and the potential effects of isoflurane. Similar studies with PET ligands have been performed for the dopamine system to closely examine the effects of endogenous neurotransmitter on radioligand binding (Delforge *et al*, 2001). Without these experiments, we are left to speculate that the effects of competing 5-HT will induce only small changes in these results based on the similarities in *in-vivo* behavior between [18F]mefway with [11C]WAY-100635 (Wooten *et al*, 2011*a*,*b*). Studies with [11C]WAY-100635 and [3H]WAY-100635 have shown negligible changes in binding due to increases and decreases in endogenous serotonin levels (Maeda *et al*, 2001; Rice *et al*, 2001). Further, our previous *in-vitro* work revealed that inhibition by 5-HT was similar for mefway (Saigal *et al*, 2006) and WAY-100635 (Khawaja *et al*, 1995).

In summary, we have made *in-vivo* measurements of K_1, V_{ND}, k_{on}, k_{off}, and B_{max} for [18F]mefway in various 5-HT_{1A} regions of the rhesus monkey brain using PET. Experiment design optimized the identifiability of the binding parameters k_{on}, k_{off}, and B_{max} to improve precision in parameter estimates. These results show that M-I [18F]mefway PET experiments can be used to measure 5-HT_{1A} receptor density across the regions of the brain. Further simplifications could be made to the M-I protocol if the desired outcome metric is limited to only B_{max} assay, which may be of value for investigating diseases or mechanisms targeting 5-HT_{1A} receptor density.

Acknowledgements

The authors would like to thank the following for their contribution to this research: Dr Jonathan Engle and Professor R Jerry Nickles for assistance with isotope production; Julie Larson and the staff at the Harlow Center for Biological Psychology at the University of Wisconsin for nonhuman primate handling; Dr Alex Converse and Professor Jim Holden for technical discussions; Dr Suresh Pandey and Neil Saigal for providing the *trans*-tosyl mefway precursor.

Disclosure/conflict of interest

The authors declare no conflict of interest.

References

Bacopoulos NG, Redmond DE, Roth RH (1979) Serotonin and dopamine metabolites in brain regions and cerebrospinal fluid of primate species: effects of ketamine and fluphenazine. *J Neurochem* 32:1215–8

Burnet PWJ, Eastwood SL, Harrison PJ (1997) [3H]WAY-100635 for 5-HT_{1A} receptor autoradiography in human

brain: a comparison with [3H]8-OH-DPAT and demonstration of increased binding in the frontal cortex in schizophrenia. *Neurochem Int* 30:565–74

Carson RE, Lang L, Watabe H, Der MG, Adams HR, Jagoda E (2000) PET evaluation of [18F]FCWAY, an analog of the 5-HT_{1A} receptor antagonist, WAY-100635. *Nucl Med Biol* 27:493–7

Christian BT, Narayanan T, Shi B, Morris ED, Mantil J, Mukherjee J (2004) Measuring the *in vivo* binding parameters of [18F]-fallypride in monkeys using a PET multiple-injection protocol. *J Cereb Blood Flow Metab* 24:309–22

Christian BT, Vandehey NT, Floberg JM, Mistretta CA (2010) Dynamic PET denoising with HYPR processing. *J Nucl Med* 51:1147–54

Costes N, Merlet I, Zimmer L, Lavenne F, Cinotti L, Delforge J, Luxen A, Pujol J-F, Le Bars D (2002) Modeling [18F]MPPF positron emission tomography kinetics for the determination of 5-hydroxytryptamine(1A) receptor concentration with multiinjection. *J Cereb Blood Flow Metab* 22:753–65

Delforge J, Bottlaender M, Loc'h C, Guenther I, Fuseau C, Bendriem B, Syrota A, Mazière B (1999) Quantitation of extrastriatal D_2 receptors using a very high-affinity ligand (FLB 457) and the multi-injection approach. *J Cereb Blood Flow Metab* 19:533–46

Delforge J, Bottlaender M, Pappata S, Loc'h C, Syrota A (2001) Absolute quantification by positron emission tomography of the endogenous ligand. *J Cereb Blood Flow Metab* 21:613–30

Delforge J, Spelle L, Bendriem B, Samson Y, Bottlaender M, Papageorgiou S, Syrota A (1996) Quantitation of benzodiazepine receptors in human brain using the partial saturation method. *J Nucl Med* 37:5–11

Delforge J, Syrota A, Mazoyer BM (1990) Identifiability analysis and parameter identification of an *in vivo* ligand-receptor model from PET data. *IEEE Trans Biomed Eng* 37:653–61

Druse MJ, Kuo A, Tajuddin N (1991) Effects of in utero ethanol exposure on the developing serotonergic system. *Alcohol Clin Exp Res* 15:678–84

Farde L, Ginovart N, Ito H, Lundkvist C, Pike VW, McCarron JA, Halldin C (1997) PET-characterization of [carbonyl-11C]WAY-100635 binding to 5-HT_{1A} receptors in the primate brain. *Psychopharmacology* 133:196–202

Gallezot J-D, Bottlaender MA, Delforge J, Valette H, Saba W, Dollé F, Coulon CM, Ottaviani MP, Hinnen F, Syrota A, Grégoire M-C (2008) Quantification of cerebral nicotinic acetylcholine receptors by PET using 2-[18F]fluoro-A-85380 and the multiinjection approach. *J Cereb Blood Flow Metab* 28:172–89

Gunn RN, Sargent PA, Bench CJ, Rabiner EA, Osman S, Pike VW, Hume SP, Grasby PM, Lammertsma AA (1998) Tracer kinetic modeling of the 5-HT_{1A} receptor ligand [carbonyl-11C]WAY-100635 for PET. *Neuroimage* 8:426–40

Hall H, Lundkvist C, Halldin C, Farde L, Pike VW, McCarron JA, Fletcher A, Cliffe IA, Barf T, Wikström H, Sedvall G (1997) Autoradiographic localization of 5-HT_{1A} receptors in the post-mortem human brain using [3H]WAY-100635 and [11C]WAY-100635. *Brain Res* 745:96–108

Holden JE, Doudet DJ (2004) Positron emission tomography receptor assay with multiple ligand concentrations: an equilibrium approach. In: *Methods in enzymology* (Abelson JN, Simon MI, eds), vol. 385. New York: Academic Press, 169–84

Innis RB, Cunningham VJ, Delforge J, Fujita M, Gjedde A, Gunn RN, Holden J, Houle S, Huang S-C, Ichise M, Iida H, Ito H, Kimura Y, Koeppe RA, Knudsen GM, Knuuti J, Lammertsma AA, Laruelle M, Logan J, Maguire RP, Mintun MA, Morris ED, Parsey R, Price JC, Slifstein M, Sossi V, Suhara T, Votaw JR, Wong DF, Carson RE (2007) Consensus nomenclature for *in vivo* imaging of reversibly binding radioligands. *J Cereb Blood Flow Metab* 27:1533–9

Khawaja X, Evans N, Reilly Y, Ennis C, Minchin MCW (1995) Characterization of the binding of [3H]WAY-100635, a novel 5-hydroxytryptamine$_{1A}$ receptor antagonist, to rat brain. *J Neurochem* 64:2716–26

Köhler C, Radesäter A-C, Lang W, Chan-Palay V (1986) Distribution of serotonin-1A receptors in the monkey and the postmortem human hippocampal region. A quantitative autoradiographic study using the selective agonist [3H]8-OH-DPAT. *Neurosci Lett* 72:43–8

Lang L, Jagoda E, Schmall B, Sassaman M, Magata Y, Eckelman WC (1999) Comparison of F-18 labeled cis and trans 4-fluorocyclohexane derivatives of WAY 100635. *J Nucl Med* 40:37P–8P

Le Bars D, Lemaire C, Ginovart N, Plenevaux A, Aerts J, Brihaye C, Hassoun W, Leviel V, Mekhsian P, Weissmann D, Pujol JF, Luxen A, Comar D (1998) High-yield radiosynthesis and preliminary *in vivo* evaluation of p-[18F]MPPF, a fluoro analog of WAY-100635. *Nucl Med Biol* 25:343–50

Logan J, Fowler JS, Volkow ND, Ding YS, Wang G-J, Alexoff DL (2001) A strategy for removing the bias in the graphical analysis method. *J Cereb Blood Flow Metab* 21:307–20

Logan J, Fowler JS, Volkow ND, Wang GJ, Ding YS, Alexoff DL (1996) Distribution volume ratios without blood sampling from graphical analysis of PET data. *J Cereb Blood Flow Metab* 16:834–40

Logan J, Volkow ND, Fowler JS, Wang GJ, Dewey SL, MacGregor R, Schlyer D, Gatley SJ, Pappas N, King P, Hitzemann R, Vitkun S (1994) Effects of blood flow on [nC]raclopride binding in the brain: model simulations and kinetic analysis of PET data. *J Cereb Blood Flow Metab* 14:995–1010

Logan J, Volkow ND, Fowler JS, Wang G-J, Fischman MW, Foltin RW, Abumrad NN, Vitkun S, Gatley SJ, Pappas N, Hitzemann R, Shea CE (1997) Concentration and occupancy of dopamine transporters in cocaine abusers with [11C]cocaine and PET. *Synapse* 27:347–56

Maeda J, Suhara T, Ogawa M, Okauchi T, Kawabe K, Zhang MR, Semba J, Suzuki K (2001) *In vivo* binding properties of [carbonyl-11C]WAY-100635: effect of endogenous serotonin. *Synapse* 40:122–9

Mauger G, Saba W, Hantraye P, Dolle F, Coulon C, Bramoulle Y, Chalon S, Grégoire M-C (2005) Multiinjection approach for D_2 receptor binding quantification in living rats using [11C]raclopride and the b-microprobe: crossvalidation with *in vitro* binding data. *J Cereb Blood Flow Metab* 25:1517–27

Morris ED, Babich JW, Alpert NM, Bonab AA, Livni E, Weise S, Hsu H, Christian BT, Madras BK, Fischman AJ (1996) Quantification of dopamine transporter density in monkeys by dynamic PET imaging of multiple injections of [11C]-CFT. *Synapse* 24:262–72

Morris ED, Bonab AA, Alpert NM, Fischman AJ, Madras BK, Christian BT (1999) Concentration of dopamine transporters: to B_{max} or not to B_{max}? *Synapse* 32:136–40

Morris ED, Christian BT, Yoder KK, Muzic RF (2004) Estimation of local receptor density, B'max, and other

parameters via multiple-injection positron emission tomography experiments. In: *Methods in enzymology* (Abelson JN, Simon MI, eds), vol. 385. New York: Academic Press, 184–213

Muzic RF, Christian BT (2006) Evaluation of objective functions for estimation of kinetic parameters. *Med Phys* 33:342–53

Muzic RF, Cornelius S (2001) COMKAT: compartment model kinetic analysis tool. *J Nucl Med* 42:636–45

Muzic RF, Saidel GM, Zhu N, Nelson AD, Zheng L, Berridge MS (2000) Iterative optimal design of PET experiments for estimating β-adrenergic receptor concentration. *Med Biol Eng* 38:593–602

Olsson H, Halldin C, Farde L (2004) Differentiation of extrastriatal dopamine D2 receptor density and affinity in the human brain using PET. *Neuroimage* 22:794–803

Pike VW, McCarron JA, Lammertsma AA, Osman AA, Hume SP, Sargent PA, Bench CJ, Cliffe IA, Fletcher A, Grasby PM (1996) Exquisite delineation of 5-HT_{1A} receptors in human brain with PET and [carbonyl-^{11}C]-WAY-100635. *Eur J Pharmacol* 301:R5–7

Poyot T, Condé F, Grégoire M-C, Frouin V, Coulon C, Fuseau C, Hinnen F, Dollé F, Hantraye P, Bottlaender M (2001) Anatomic and biochemical correlates of the dopamine transporter ligand [^{11}C]-PE2I in normal and parkinsonian primates: comparison with 6-[^{18}F]fluoro-L-DOPA. *J Cereb Blood Flow Metab* 21:782–92

Rice OV, Gatley SJ, Shen J, Huemmer CL, Rogoz R, DeJesus OT, Volkow ND, Gifford AN (2001) Effects of endogenous neurotransmitters on the *in vivo* binding of dopamine and 5-HT radiotracers in mice. *Neuropsychopharmacology* 25:679–89

Saigal N, Pichika R, Easwaramoorthy B, Collins D, Christian BT, Shi B, Narayanan TK, Potkin SG, Mukherjee J (2006) Synthesis and biologic evaluation of a novel serotonin 5-HT_{1A} receptor radioligand, [^{18}F]-labeled mefway, in rodents and imaging by PET in a nonhuman primate. *J Nucl Med* 47:1697–706

Salinas C, Muzic RF, Ernsberger P, Saidel GM (2007) Robust experiment design for estimating myocardial beta adrenergic receptor concentration using PET. *Med Phys* 34:151–65

Spinelli S, Chefer S, Carson RE, Jagoda E, Lang L, Heilig M, Barr CS, Suomi SJ, Higley JD, Stein EA (2010) Effects of early-life stress on serotonin$_{1A}$ receptors in juvenile rhesus monkeys measured by positron emission tomography. *Biol Psychiatry* 67:1146–53

Tai YC, Chatziioanno A, Siegel S, Young J, Newport D, Goble RN, Nutt RE, Cherry SR (2001) Performance evaluation of the microPET P4: a PET system dedicated to animal imaging. *Phys Med Biol* 46:1845–62

Tokugawa J, Ravasi L, Nakayama T, Lang L, Schmidt KC, Seidel J, Green MV, Sokoloff L, Eckelman WC (2007) Distribution of the 5-HT_{1A} receptor antagonist [^{18}F]-FPWAY in blood and brain of the rat with and without isoflurane anesthesia. *Eur J Nucl Med Mol Imaging* 34:259–66

Vandehey NT, Moirano JM, Converse AK, Holden JE, Mukherjee J, Murali D, Nickles RJ, Davidson RJ, Schneider ML, Christian BT (2010) High-affinity dopamine D_2/D_3 PET radioligands [^{18}F]-fallypride and [^{11}C]-FLB457: a comparison of kinetics in extrastriatal regions using a multiple-injection protocol. *J Cereb Blood Flow Metab* 30:994–1007

Wilson AA, Garcia A, Li J, Dasilva JN, Houle S (1999) Analogues of WAY-100635 as radiotracers for *in vivo* imaging of 5-HT_{1A} receptors. *J Labelled Compd Rad* 42:611–20

Wooten DW, Hillmer AT, Murali D, Barnhart TE, Schneider ML, Mukherjee J, Christian BT (2011*b*) An *in vivo* comparison of *cis*- and *trans*-[^{18}F]mefway in the nonhuman primate. *Nucl Med Biol* 38:925–32

Wooten DW, Moraino JM, Hillmer AT, Engle JW, DeJesus OT, Murali D, Barnhart TE, Nickles RJ, Davidson R, Schneider ML, Mukherjee J, Christian BT (2011*a*) *In vivo* kinetics of [^{18}F]MEFWAY: a comparison with [^{11}C]WAY-100635 and [^{18}F]MPPF in the nonhuman primate. *Synapse* 65:592–600

Supplementary Information accompanies the paper on the Journal of Cerebral Blood Flow & Metabolism website (http://www.nature.com/jcbfm)